Chemistry and phase petrology of amphiboles and orthoamphibole–cordierite rocks, Old Woman Mountains, SE California, USA

EDWARD F. STODDARD[1] AND CALVIN F. MILLER[2]
[1]Department of Marine, Earth and Atmospheric Sciences, North Carolina State University, Raleigh, NC 27695-8208, USA
[2]Department of Geology, Vanderbilt University, Nashville, TN 37235, USA

Abstract

Proterozoic amphibolites from Sweetwater Wash, in the Old Woman Mountains of southeastern California, contain a variety of mineral assemblages dominated by the low-Ca amphiboles anthophyllite, gedrite, and cummingtonite. Their Mg- and Al-rich, Ca-poor bulk compositions suggest that the amphibolites represent basalts that were altered prior to metamorphism. In addition to amphiboles, mineral assemblages include cordierite, biotite, garnet, Ca-rich plagioclase, and ilmenite ± rutile. Corundum, staurolite, and spinel occur locally in Al-rich enclaves associated with cordierite. Orthoamphiboles commonly exhibit complex microstructures, including twinning, intergrowths, and apparent exsolution; spot analyses show an unusually large range of chemical compositions, even within a single thin section, in several cases extending across the crest of the solvus in the orthoamphibole system. Ionic substitution within the orthoamphibole series was dominated by the Mg-tschermakitic and edenitic exchange reactions. The amphibolites are thought to have been subjected to metamorphic temperatures above the orthoamphibole solvus during both the Proterozoic and the Cretaceous. Cretaceous metamorphism was followed closely by rapid uplift and denudation, which may be responsible for the exsolution and range of compositions of the orthoamphiboles.

KEYWORDS: amphibolite, amphibole, orthoamphibole, cordierite, Old Woman Mountains, California.

Introduction

THE Old Woman–Piute Range is a north–south trending mountain range located in the eastern Mojave Desert, about 70 km west of Needles, California (Fig. 1). The geology of the range is characterized by three groups of older metamorphic rocks which were intruded by late Mesozoic granitoid plutons and are overlain by Cenozoic volcanic and sedimentary rocks (Miller *et al.*, 1982). The metamorphic rocks include a sequence that is the metamorphosed equivalent of the Cambrian to Triassic stratigraphic section typical of the western Colorado Plateau and eastern Mojave Desert (Stone *et al.*, 1983). It is dominated here by marble, with subordinate quartzite, pelitic schist, and calc-silicate rock. Precambrian rocks can be divided into an older series that was metamorphosed at high grade prior to 1.68 Ga, and a younger series ($\leq$1.68 Ga), which was not strongly metamorphosed prior to the Mesozoic. The older series includes both supracrustal rocks (now paragneisses, schists, and amphibolites) and plutonic rocks which intrude the supracrustals. The younger series comprises the 1.68 Ga Fenner batholith (Bender and Miller, 1987), 1.42 Ga syenites (Gleason *et al.*, 1988) and diabase dykes whose probable age is 1.1 to 1.2 Ga.

This paper is concerned with a group of Proterozoic metamorphic rocks exposed in Sweetwater Wash, in the north-central Old Woman Mountains (Fig. 2). Here, amphibolites and other supracrustal rocks of the older Proterozoic series are interlayered within a two-km thick screen that separates the overlying Sweetwater Wash two-mica granite pluton from the underlying Old Woman hornblende–biotite granodiorite pluton. Both plutons are approximately 74 Ma (Foster *et al.*, 1989) and are late syn- to post-Mesozoic metamorphism and deformation. Dykes and sills of Sweetwater Wash granite inject the screen extensively. Rocks exposed within the screen

Mineralogical Magazine, September 1990, Vol. 54, pp. 393–406

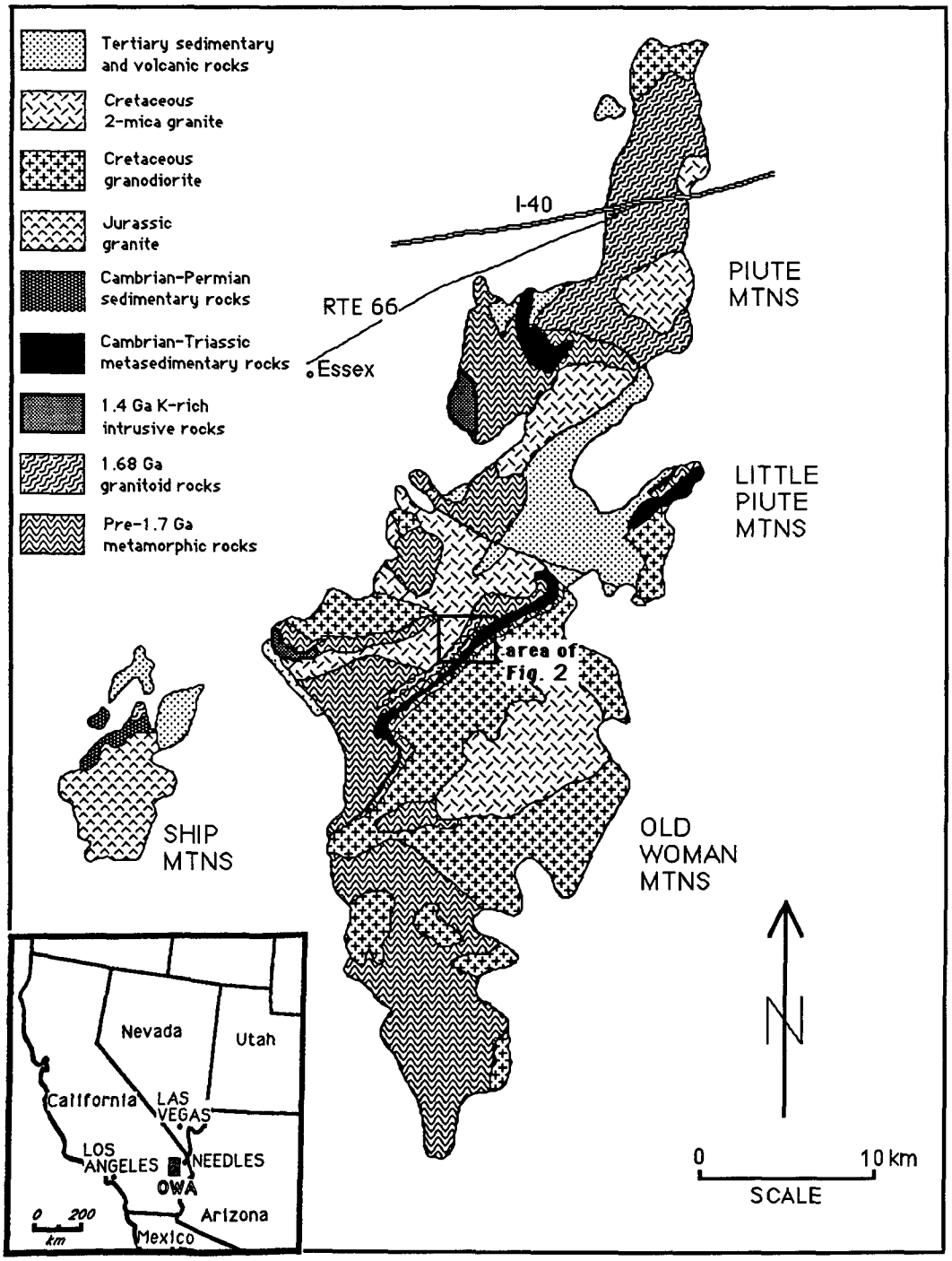

FIG. 1. Location and general geology of the study area (OWA = Old Woman Mountains).

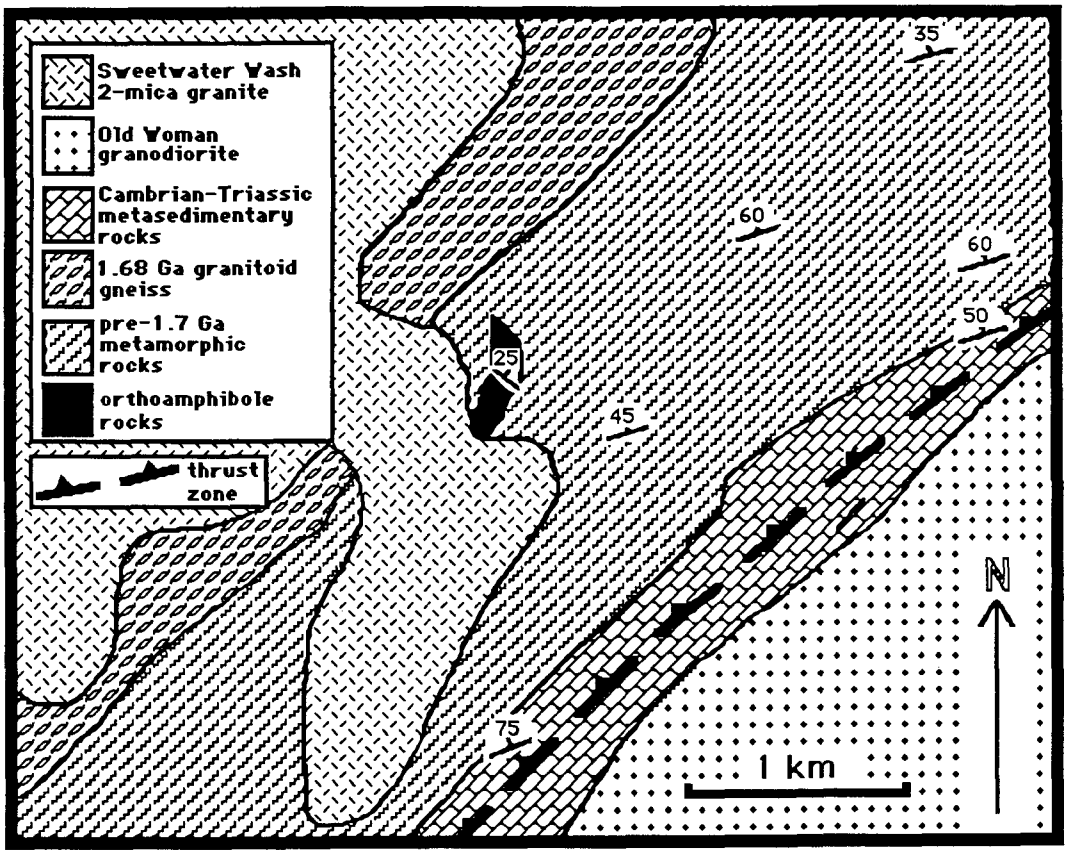

FIG. 2. Geology of Sweetwater Wash area, showing location of orthoamphibole-bearing and other rocks.

include both older and younger series Proterozoic orthogneisses and Palaeozoic metasedimentary rocks in addition to the older Proterozoic supracrustal rocks. The inverted Proterozoic and Cambrian rocks constitute the upper plate of a major ductile thrust that emplaced them above upright upper Palaeozoic rocks (Miller *et al.*, 1982; Howard *et al.*, 1987). Rocks within the screen generally strike northeast and dip northwest, but attitudes show considerable local variation as a result of complex folding.

The older metamorphic rocks within the screen have had a very complex history. They underwent very high-grade metamorphism prior to 1.68 Ga. The presence of relict orthopyroxene in garnet amphibolite and quartzofeldspathic gneiss in and just north of Sweetwater Wash suggests that granulite facies conditions were attained at least locally in this area, as they were in other parts of the Colorado River region (e.g. Thomas *et al.*, 1988). Early kyanite that we have observed in several thin sections of older Proterozoic rocks from in and around Sweetwater Wash may indicate a relatively high-P Proterozoic cooling path or, perhaps more likely, an early, relatively high-P, low-T phase of Mesozoic metamorphism.

Peak Mesozoic grade, indicated by sillimanite + K-feldspar + muscovite assemblages in the metamorphosed equivalent of the Cambrian Bright Angel Shale, was upper-amphibolite facies (Miller *et al.*, 1982; Hoisch *et al.*, 1988). Pressures at the time of granitoid emplacement are estimated to have been near 6 kbar (Foster *et al.*, 1989; Young and Wooden, 1988). Late andalusite in older Proterozoic series rocks suggests a steep dP/dT during cooling; this is consistent with the extremely rapid Late Cretaceous unroofing of this area implied by $^{40}Ar/^{39}Ar$ data (e.g. Foster *et al.*, 1989).

The amphibolites that we studied are exposed on the west side of a low ridge that borders on the east side of Sweetwater Wash. They strike

TABLE 1. MINERAL ASSEMBLAGES

samp#	type[1]	cr[2]	an	gd	cm	hb	ga	bi	pl[3]	qz	rt	cn	st	sp	il	ch	px	tn
W29D	4	X	X		?			X	X		X				X			
W223	4	X	X	?			X	X	X	X		X	X	X	X			
W127	4		?	X	?		X	X	68	X					X	?		
W145	4	X		X				X	X						X	X		
Wan	4	X	X		?			X	X		X				X			
5XX	4	X	X	X				X	88	X		X	X	X	X			
5A2	4	X	X		?			X	X		X				X			
5A3	4		?	X	X		X	X	85	X					X			
W29	3						X	?	X				X		X	X		
W29B	1				X	X	X	X	88	X					X			
W29C	2				X	X											X	X

[1]refers to petrographic variety of amphibolite (see text)
[2]abbreviations: cr, cordierite; an, anthophyllite; gd, gedrite; cm, cummingtonite; hb, hornblende; ga, garnet; bi, biotite; pl, plagioclase; qz, quartz; rt, rutile; cn, corundum; st, staurolite; sp, spinel; il, ilmenite; ch, chlorite; px, clinopyroxene; tn, titanite
[3]An content listed where measured

northwest and dip northeast, contrary to the general northeast striking, northwest-dipping attitudes within the screen. We have traced them for less than 200 m along strike, and the structural thickness over which they are exposed is less than 50 m. Lithologic units within the amphibolite package are interlayered on scales from about one metre down to about five cm. The distinct lithologic types that we have identified include: (1) 'normal' hornblende-plagioclase amphibolite; (2) sparse clinopyroxene-rich, hornblende + epidote + titanite-bearing amphibolite; (3) chlorite-rich, apparently altered rocks; and (4) abundant orthoamphibole-bearing rocks with and without cordierite. Table 1 lists complete mineral assemblages for samples of each of the four types. This paper focusses on the fourth type of amphibolite; the first three will be considered only briefly.

Rock chemistry and protolith

Eight rocks were analysed (X-ray fluorescence spectrometry) for major and selected minor elements. Analysed samples included four of the orthoamphibole-rich rocks (type 4), two of the hornblende–plagioclase amphibolites (type 1) and one each of the other two petrographic varieties. The major-element chemistry (Fig. 3) of the four amphibolite varieties is extremely variable; for example, SiO_2 ranges from 41.9 to 60.9 wt.% (totals normalized on a volatile-free basis to 100%), and CaO ranges from 0.5 to 17 wt.%. However, the more stable minor elements analysed are quite consistent among the samples. For example, TiO_2 ranges only from about 0.9 to 1.2 wt.%. The stable minor and trace elements, as well as the field occurrence (interstratified with pelitic to semipelitic paragneiss and schist), are more consistent with an origin as basaltic lavas, rather than as sedimentary rocks (cf. Reinhardt, 1987).

On a CaO–Fe_2O_3*–MgO ternary plot, the Fe_2O_3*/MgO ratio remains relatively constant for all analysed samples, but CaO shows a great range (Fig. 3). The relationship between the mineral assemblages and the rock chemistry is clear: the Ca-poor rocks are also the hornblende-free rocks. The Ca-poor chlorite-rich rocks may be altered equivalents of the orthoamphibole-bearing rocks, while the clinopyroxene-rich amphibolites are the richest in CaO. We believe that these rocks may have originated as basalts that were subjected to intense hydrothermal alteration prior to metamorphism, and that the apparently high mobility of Ca under these conditions thus exerted the controlling influence on their mineralogy after metamorphism. Such an origin for cordierite–orthoamphibole rocks has been suggested elsewhere by Vallance (1967).

Petrography of orthoamphibole rocks

In many of the orthoamphibole-bearing rocks (samples Wan, 5XX, 5A2, W223; see Table 1), the orthoamphibole and cordierite each constitute 40 to 50% of the sample, while the other mineral phases are minor. The remaining specimens are more quartzofeldspathic, and while all specimens contain at least some biotite, it is sparse in all except W145, which is actually an orthoamphibole–biotite schist. All samples contain at least one Ti-rich phase (ilmenite and/or rutile). Garnet and orthoamphibole coexist in two cordierite-free specimens (5A3, W127); in sample W223 garnet is present as inclusions in cordierite, and not in contact with orthoamphibole. Cordierite and cummingtonite appear to be mutually exclusive. Staurolite, green spinel, and corundum are present only within Al-rich 'enclaves' (Robinson and

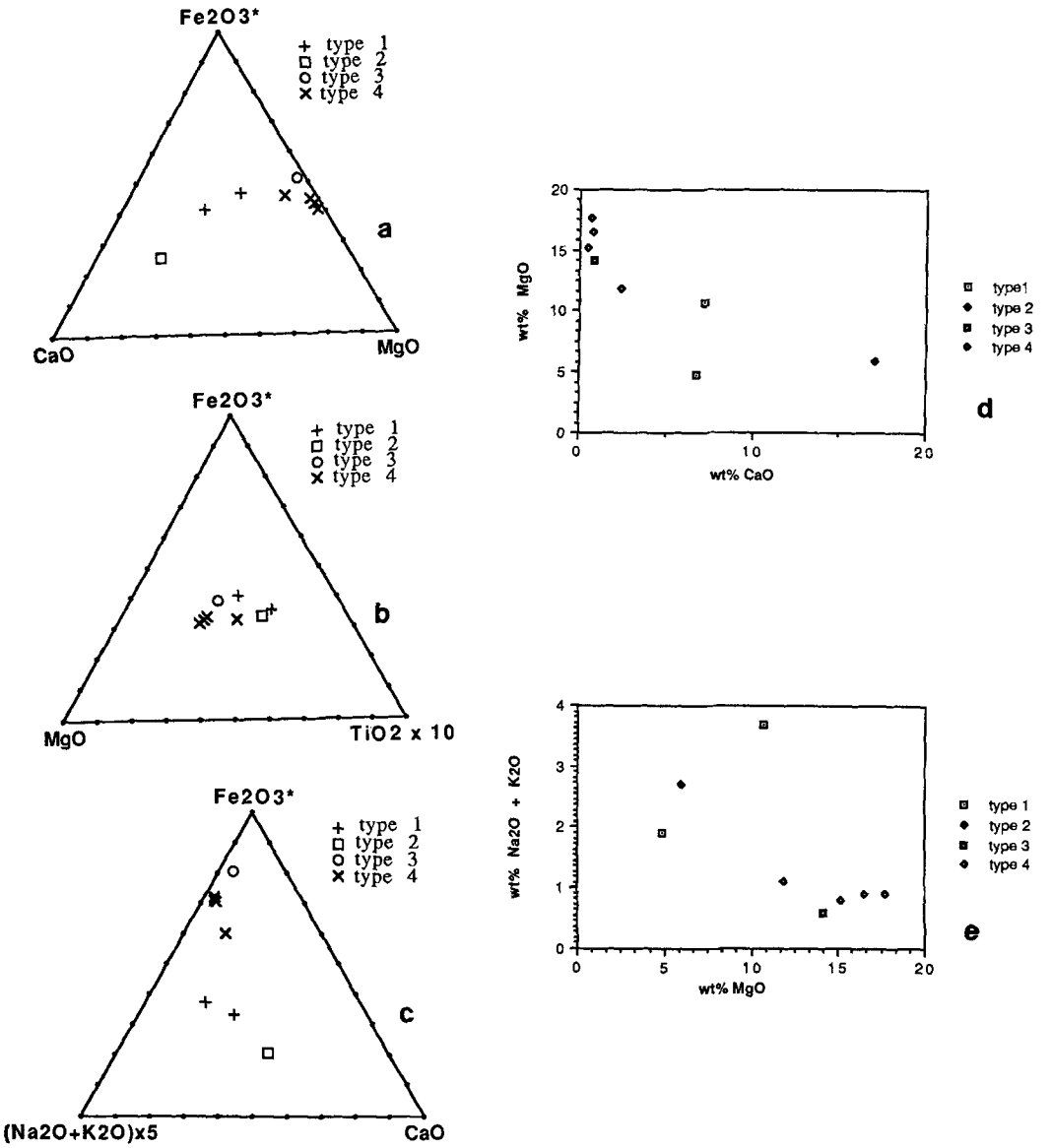

FIG. 3. Plots of selected oxides from whole-rock analyses of amphibolites. Analyses were first normalized to 100% on a volatile-free basis. Oxides plotted on ternary diagrams (3*a*, 3*b*, and 3*c*) normalized to 100%. Type (1, 2, 3, or 4) refers to petrographic variety, type 4 the orthoamphibole-bearing rocks. See text for further discussion.

Jaffe, 1969; Schumacher and Robinson, 1987), associated with Ca-rich plagioclase, and enclosed within cordierite. Quartz is present in most, if not all, samples, but is exceedingly sparse in a few. Plagioclase is present in all samples, but seldom exhibits twinning, and is difficult to distinguish from quartz and cordierite. Chlorite is present as an alteration product.

Orthoamphibole (gedrite) and cummingtonite coexist as discrete, optically distinctive and generally homogeneous phases in one specimen (5A3; Fig. 4*a*). In this rock, the orthoamphibole is more abundant than cummingtonite, and occurs as larger, elongate prisms. The cummingtonite occurs as smaller, patchy, poikiloblastic grains, commonly in contact with gedrite. In a few cases,

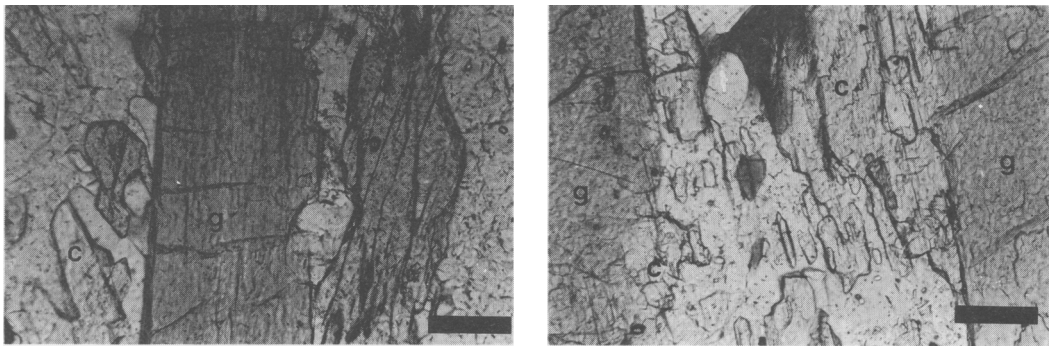

FIG. 4. Photomicrographs, under plane-polarized light from specimen 5A3: (*a*, *left*) Discrete, optically homogeneous gedrite and cummingtonite grains; (*b*, *right*) Composite grain, with both gedrite and cummingtonite. Scale bars equal 0.5 mm.

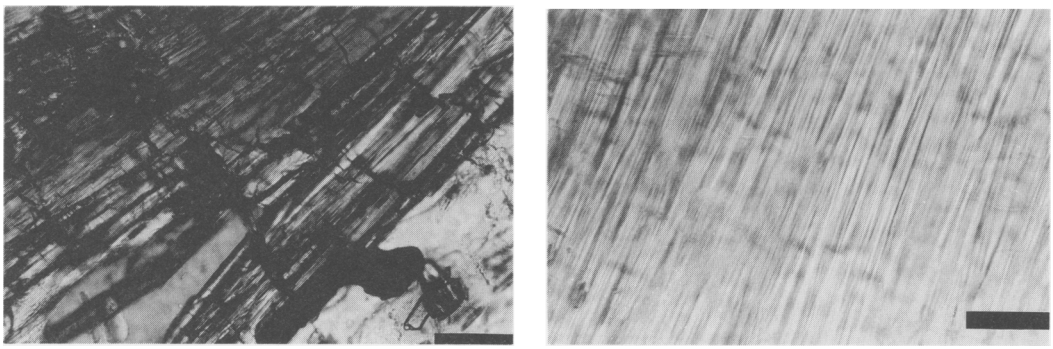

FIG. 5. Selected photomicrographs, showing complex microstructural relations of orthoamphiboles: (*a*, *left*) Fine-scale lamellar intergrowth or twinning, specimen 5XX; crossed polars, scale bar equals 0.5 mm; (*b*, *right*) Fine-scale exsolution (?) in large orthoamphibole grain, specimen 5XX; plane-polarized light, scale bar equals 0.3 mm.

the two amphiboles make up composite grains (Fig. 4*b*). Gedrite displays moderate to strong pleochroism from colourless to grey or greenish-grey; the coexisting cummingtonite is colourless, or nearly so. In this sample, the cummingtonite shows discernibly lower relief than the gedrite, and cummingtonite has slightly higher birefringence (approximately 0.026 *vs.* 0.020 for gedrite). In sample 5A3, exsolution lamellae are generally not visible in the amphiboles (Fig. 4).

In the other specimens examined, orthoamphibole relationships are complex. Most grains are twinned, exsolved, and commonly intergrown in a lamellar or patchy fashion (Fig. 5*a* and *b*). Some of the intergrowths are coarse and may represent primary two-orthoamphibole assemblages (cf. Spear, 1980), whereas finer-scale intergrowths and exsolution probably resulted from secondary or retrograde effects as discussed by Treloar and Putnis (1982). These complex microstructures are of utmost importance in interpretation of the amphibole analyses. Optically zoned orthoamphiboles, such as those described by Harley (1985) from Antarctica, were not observed.

Orthoamphibole chemistry

Analyses and recalculations. Approximately 140 spot analyses were obtained on orthoamphibole grains. By the IMA amphibole nomenclature scheme, these analyses include anthophyllite, alumino-anthophyllite, and gedrite (Rock and Leake, 1984). The analyses span a large range from nearly end-member anthophyllite, with 7.8 Si cations per formula unit (23 oxygens, anhydrous basis), to gedrite with 6.2 Si per formula unit. Even within a single sample (W127), the range of individual spot analyses is as much as 7.504 to 6.274 Si per formula unit. Table 2 lists representative analyses of orthoamphiboles. Two or three

TABLE 2. SELECTED ANTHOPHYLLITE-GEDRITE ANALYSES

Sample	Wan	Wan	W29D	W29D	W223	W223	W145	5A2	W127	W127	5XX	5XX	5XX	5A3	5A3	5A3
Grain	1A	2A	1A	3A	1A	2A	1A	1A	1A	2A	1A	2A	1B	1B	2A	2B
	weight % oxides										weight % oxides					
SiO_2	57.49	53.53	54.70	51.81	53.13	46.35	41.75	53.68	42.55	50.54	48.53	46.98	53.57	50.76	45.15	43.74
Al_2O_3	1.18	4.74	1.19	6.73	3.77	12.32	17.34	3.54	16.83	5.22	8.73	10.28	2.67	7.61	13.40	16.17
Cr_2O_3		0.12	0.06	0.06		0.10			0.06	0.02						
TiO_2	0.05	0.11	0.01	0.11	0.08	0.22	0.25	0.06	0.26	0.11	0.09	0.14	0.07	0.10	0.21	0.25
FeO	18.41	18.31	19.62	18.47	22.28	23.14	23.60	18.84	23.17	23.33	22.73	21.70	22.16	22.77	22.99	22.37
MnO	0.48	0.53	0.59	0.53	0.51	0.55	0.67	0.41	0.62	0.54	0.54	0.52	0.51	0.40	0.38	0.45
MgO	21.51	20.73	21.25	19.74	17.57	14.19	12.39	20.75	12.18	16.57	15.90	15.83	18.13	15.68	14.28	12.03
CaO	0.66	0.65	0.59	0.58	0.38	0.65	0.25	0.41	0.61	0.44	0.48	0.54	0.33	0.47	0.57	0.60
Na_2O	0.03	0.27	0.06	0.43	0.29	1.25	2.01	0.26	1.82	0.59	0.91	0.93	0.12	0.73	1.31	1.72
K_2O	0.07	0.07	0.06	0.07	0.05	0.09	0.04	0.08	0.10	0.06	0.10	0.04	0.09	0.03	0.12	0.06
ZnO								0.03	0.35	0.34	0.30	0.37			0.23	
total	99.89	99.06	98.14	98.54	98.05	98.87	98.30	98.03	98.55	97.75	98.30	97.32	97.65	98.55	98.64	97.39
T	site occupancy (per 23 oxygens on anhydrous basis)										site occupancy (per 23 oxygens on anhydrous basis)					
Si	7.975	7.534	7.818	7.348	7.685	6.753	6.173	7.647	6.274	7.434	7.092	6.919	7.775	7.338	6.607	6.456
Al^{iv}	0.025	0.466	0.182	0.652	0.315	1.247	1.827	0.353	1.726	0.566	0.908	1.081	0.225	0.662	1.393	1.544
M1,2,3,4																
Al^{vi}	0.168	0.320	0.018	0.473	0.329	0.870	1.196	0.241	1.199	0.340	0.596	0.704	0.232	0.635	0.918	1.270
Ti	0.006	0.012	0.001	0.012	0.009	0.024	0.028	0.007	0.029	0.012	0.010	0.015	0.007	0.011	0.023	0.028
Cr		0.014	0.007	0.007		0.012			0.007	0.002						
Mg	4.447	4.349	4.527	4.173	3.788	3.080	2.730	4.405	2.677	3.632	3.464	3.474	3.921	3.379	3.113	2.647
Fe	2.136	2.155	2.346	2.191	2.695	2.820	2.919	2.245	2.857	2.870	2.779	2.673	2.690	2.752	2.813	2.761
Zn								0.002	0.020	0.020	0.017	0.021			0.013	
Mn	0.056	0.063	0.072	0.063	0.062	0.068	0.084	0.050	0.077	0.067	0.067	0.065	0.062	0.049	0.048	0.056
Ca	0.099	0.098	0.091	0.089	0.058	0.102	0.040	0.057	0.096	0.069	0.075	0.085	0.051	0.072	0.089	0.095
Na	0.008				0.059	0.024	0.003		0.038				0.034	0.102		0.143
ΣM	7.000	7.011	7.062	7.008	7.000	7.000	7.000	7.007	7.000	7.012	7.008	7.037	7.000	7.000	7.017	7.000
A																
Na		0.074	0.017	0.118	0.021	0.328	0.572	0.071	0.483	0.167	0.257	0.266		0.102	0.373	0.349
K	0.012	0.013	0.012	0.013	0.009	0.017	0.007	0.015	0.018	0.011	0.018	0.007	0.016	0.005	0.023	0.011
ΣA	0.012	0.087	0.029	0.131	0.030	0.345	0.579	0.086	0.501	0.178	0.275	0.273	0.016	0.107	0.396	0.360

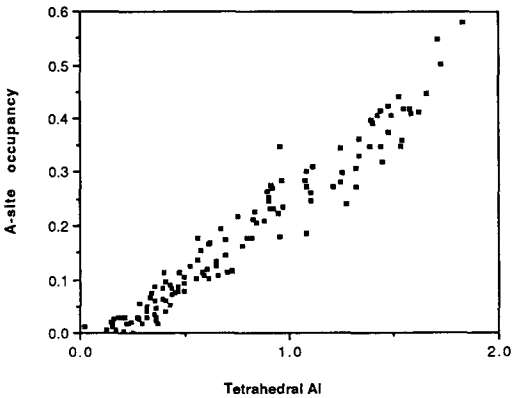

FIG. 6. Calculated *A*-site occupancy plotted against tetrahedral Al for all orthoamphibole analyses. Positive, linear trend indicates edenite substitution, but slope indicates more Al present in tetrahedral sites than can be accounted for by edenitic substitution alone.

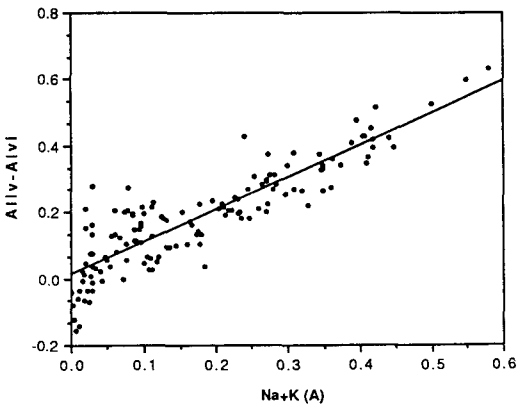

FIG. 7. Calculated *A*-site occupancy plotted against (Al^{iv}–Al^{vi}) for all orthoamphibole analyses. Linear least-squares best fit has a slope of 0.973, *y*-intercept of 0.010, and correlation coefficient of 0.781. This is interpreted as evidence that compositional variations in the orthoamphiboles analysed can be totally accounted for by edenitic and tschermakitic substitutions, allowing for analytical uncertainties.

spot analyses per section are shown in Table 2 in order to illustrate the range of orthoamphibole compositions. Interestingly, analyses made with a defocussed microprobe beam (up to 40 μm diameter) on grains that exhibit what appear to be fine-scale exsolution lamellae (Fig. 5*b*), show the same range as minimum-spot analyses.

In Table 2, no attempt has been made to estimate the ferric iron content of these amphiboles. However, ferric iron is thought to be low. Recalculations of the analyses were attempted with the assumption that all Na and K is in the *A* site, then normalizing the remaining cations to 15, and balancing the charge by adjusting the ferric/ferrous ratio ('15eNK' of Robinson *et al.*, 1982; see also Rock and Leake, 1984; Hawthorne, 1983). Using this procedure, no ferric iron could be allocated to most of the analyses, because the cation sums, excluding Na and K, are equal to or slightly less than 15, treating all Fe as ferrous. In the absence of an independent measurement of ferric/ferrous ratio in these amphiboles, or of the Na content in their *M*4 sites, it seems most likely that they have little ferric iron content. If they do, then either there are significant octahedral or tetrahedral cation site vacancies, or there are significant cations present that were not analysed.

Chemical variation and substitution mechanisms. Studies of orthoamphibole crystal chemical variations have noted that solid solution is controlled by a combination of two substitution mechanisms, one edenitic:

$$\square^{A} + Si^{IV} = Na^{A} + Al^{IV}$$

and one (Mg-) tschermakitic:

$$Mg^{VI} + Si^{IV} = Al^{VI} + Al^{IV}$$

(e.g. Berg, 1985; Robinson *et al.*, 1982). The Old Woman–Piute orthoamphiboles suggest the same effects. A plot of *A*-site occupancy versus tetrahedral Al (Fig. 6)shows a strong positive correlation, but with excess tetrahedral Al over that expected from the edenitic substitution alone. If Al enters the octahedral sites only due to the tschermakitic substitution, and enters tetrahedral sites as a result of both edenitic and tschermakitic substitution mechanisms, then a plot of (Al^{IV}–Al^{VI}) versus *A*-site occupancy (Fig. 7)should have a slope of one, and should pass through the origin, provided no other substitutions are operating. Mainly owing to the uncertainties inherent in calculating *A*-site occupancy from microprobe analyses, this plot has significant scatter; but its calculated slope (0.973), *y*-intercept (0.010), and correlation coefficient (0.781) tend to confirm that no other significant substitution mechanisms were operating.

The fact that the tschermakite substitution involved Mg and not Fe is well displayed in Fig. 8.The excellent negative correlation between Mg and octahedral Al indicates the existence of the Mg-tschermakite substitution, while Fe (*M*1, 2, 3) shows no such correlation with octahedral Al (Fig. 8). (The distribution of points on a plot of total Fe *vs.* octahedral Al is nearly identical to

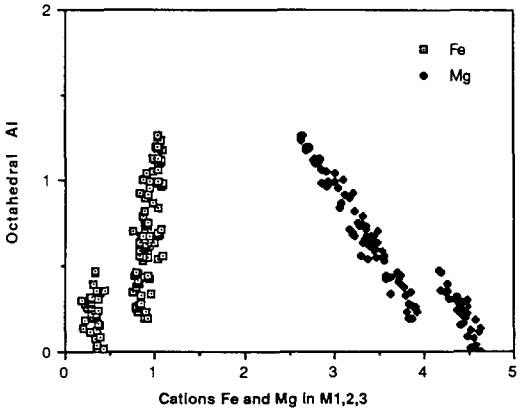

FIG. 8. Calculated number of cations of Mg (solid diamonds) and Fe (open boxes) in *M*1, *M*2, and *M*3 octahedral sites of orthoamphiboles, plotted against octahedral Al. Negative correlation of Mg with Al^{vi} demonstrates Mg-tschermak substitution. Orthoamphiboles have a continuous range of Mg contents, but fall into two distinct groups in terms of their Fe contents in *M*1, 2, 3.

that of Fe (*M*1, 2, 3) shown on Fig. 8.) Instead, the very weak positive correlation in Fig. 8 is due to the inverse relationship between Fe and Mg in the (*M*1, 2, 3) octahedral sites.

An interesting feature of Fig. 8 is the fact that the analysed orthoamphiboles separate into two very distinct compositional groups. Their Mg and Al^{vi} contents grade continuously, from 2.637 to 4.671 cations per formula unit for Mg, and from 0.018 to 1.270 for Al^{vi}. However, they are distinguished on the basis of their Mg/Al^{vi}, as shown in Fig. 8; in addition, the two populations of amphiboles have markedly different Fe contents, one group ranging from 2.040 to 2.346 Fe cations, and the other from 2.592 to 2.989 cations per formula unit. Although a crystal chemical cause cannot be ruled out on the basis of the available data, this gap in Fe contents is believed to be the result of bulk chemical differences among samples, as the high-Mg amphiboles (all anthophyllites) are from three samples (5A2, W29D, and Wan), while the lower-Mg points (including both anthophyllites and gedrites) belong to the other specimens. Orthoamphiboles analysed by Stout (1972) and by James *et al.* (1978) have Fe/Mg ratios that fall in the 'gap' of the Old Woman–Piute analyses.

In terms of other cations, the amphiboles display increasing Ti content with increasing edenite and tschermakite substitution. The Ti contents are low, however, and the substitution mechanism(s) is (are) unknown. Mn, Cr, and Zn are fairly consistent and do not appear to partition strongly between anthophyllite and gedrite.

Orthoamphibole solvus

Spear (1980; see also Robinson *et al.*, 1971, 1982; Crowley and Spear, 1981) has attempted to delineate the miscibility gap in the orthoamphibole series through compilation of available analyses. He suggests that the crest of the solvus lies at about 600°C, and at an orthoamphibole composition with $Al^{IV} = 0.75$, $Al^{VI} = 0.3$, and *A*-site occupancy of about 0.15, and that the solvus is somewhat steeper on the anthophyllite limb than on the gedrite limb. Spear (1980) also suggests that the crest of the orthoamphibole solvus rises to higher temperatures for Fe-rich compositions. Although Crowley and Spear (1981) inferred a 'positive dP/dT for the critical curve', rapid 'near-isothermal decompression' (Harley, 1985), from about 8 kbar to 5 kbar, at 650 to 700°C, did not result in any discernible exsolution for Antarctic orthoamphiboles, suggesting that the critical temperature is probably relatively pressure-insensitive through this range.

Temperatures experienced by the Old Woman Mountains orthoamphibole rocks exceeded 600° by a considerable margin both during the Early Proterozoic and during the Cretaceous. Thus, there is the possibility of crystallization of supersolvus amphibole in two discrete events, as well as for exsolution during cooling. In fact, the complex textural and compositional relations, absence of optically distinct, physically discrete coexisting pairs of orthoamphiboles, and widespread exsolution are broadly consistent with such a sequence of events.

Though they are not concentrically zoned, compositions of orthoamphiboles from most samples display continuous variation, without a pronounced gap. Only one specimen (5XX) displays a gap in compositions that coincides approximately to the crest of the solvus proposed by Spear (1980) and thus may possibly represent a primary two-orthoamphibole assemblage. Three other specimens (W127, W223, and 5A3) may contain two-phase orthoamphibole assemblages, but the data are not as clear. Three other specimens have only one variety of orthoamphibole: 5A2 and Wan contain anthophyllite only, while W145 contains only gedrite. Fig. 9 illustrates the situation.

If all these specimens had amphiboles that originally were crystallized above the solvus during the Mesozoic (and/or Proterozoic), then the present chemical variations must be due to small-scale exsolution, and many of the spot analyses may represent two-phase mixtures. In this case, the

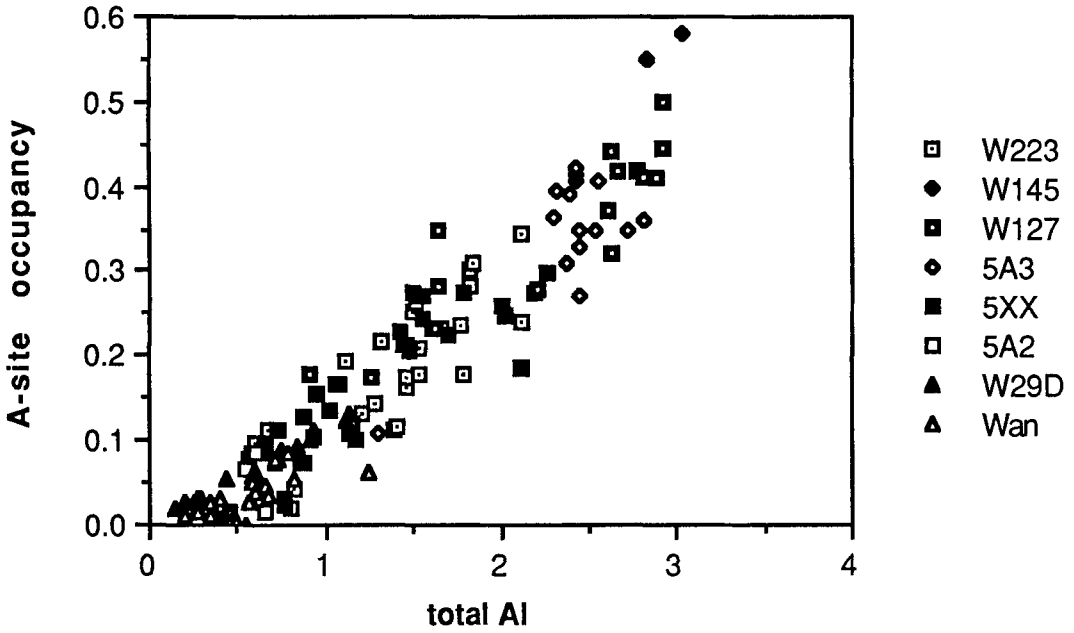

FIG. 9. Compositions of orthoamphiboles plotted in terms of their *A*-site occupancy and total Al content. Each specimen is indicated by a different symbol. Note that compositions extend across the crest of the orthoamphibole solvus, which occurs at an *A*-site occupancy of 0.15 and total Al content of about 1.05 at 600°C (Spear, 1980). Possible gaps in compositional ranges of analyses from four different specimens (5XX, W223, W127, and 5A3) do not coincide.

extreme compositions (Al-poorest anthophyllite composition and Al-richest gedrite composition from the same specimen) may indicate the conditions at which exsolution ceased during rapid regional uplift and cooling. For samples containing originally supersolvus orthoamphiboles that are presumed to have encountered the solvus during cooling, their extreme compositions correspond to temperatures between 500 and 600° on the solvus of Spear (1980). Using other criteria, it has been determined that these rocks probably cooled from temperatures above 600° to below 400° within about two million years (Foster *et al.*, 1989). This brief period may have been insufficient to allow development of simple, orderly exsolution textures and compositions, and exsolution may have been terminated at a relatively high temperature because of sluggish diffusion compared to the time available.

The data do not provide clear-cut evidence of the variation of the solvus as a function of Fe/Mg (Fig. 10). A wide range of Fe/Mg ratios is represented by the orthoamphiboles, but the Mg-richest orthoamphiboles, from samples 5A2, Wan, and W29D are all anthophyllites. The other, more Fe-rich, samples include both anthophyllite and gedrite. As noted above, because of the gap in its orthoamphibole compositions, sample 5XX may be subsolvus, but its amphiboles are Fe-poorer, not Fe-richer, than those of the other gedrite-bearing specimens. Thus it does not appear that the Mg-rich Old Woman samples are supersolvus, while the Fe-rich ones are subsolvus, as suggested by Robinson *et al.* (1982, p. 66).

Clinoamphiboles

Cummingtonite was analysed from two samples: 5A3, in which it coexists with gedrite, and W29B, in which it coexists with hornblende. Table 3 shows analyses of cummingtonite and hornblende. Coexisting pairs of anthophyllite and cummingtonite have not been observed, but the compositions of the analysed cummingtonites generally overlap with the compositions of the anthophyllites from other samples. Comparing the analysed cummingtonites with anthophyllites of similar Al content, there is a suggestion that the cummingtonite is slightly enriched in Ca and K compared with anthophyllite. Hornblende par-

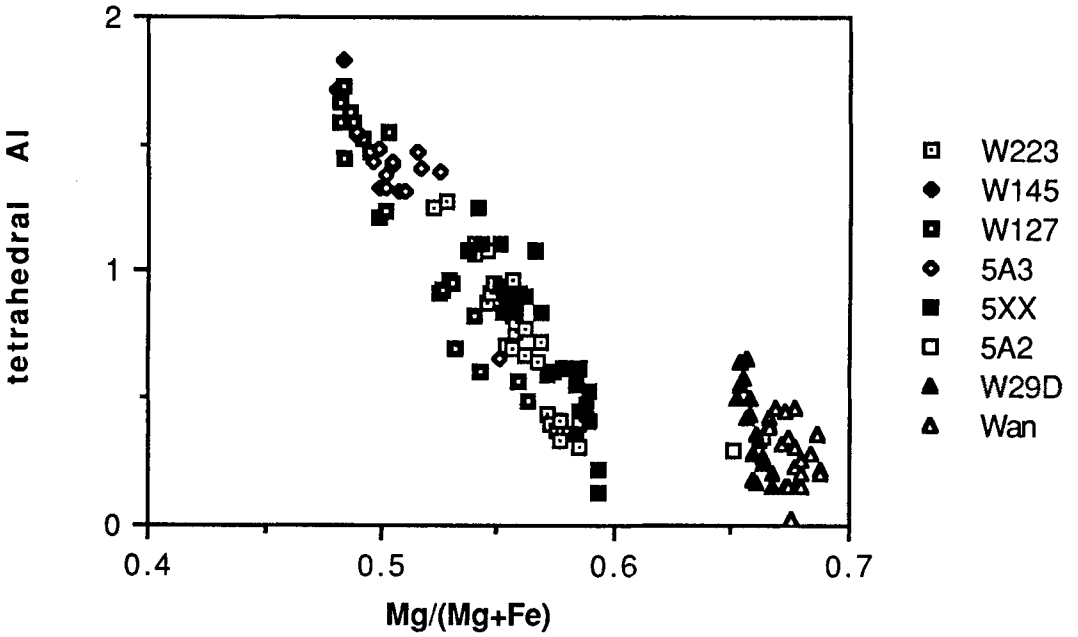

FIG. 10. Tetrahedral Al content plotted against Mg/(Mg + Fe) for all orthoamphibole analyses. Three specimens (5A2, Wan, and W29D) have higher Mg/Fe than the others; anthophyllites from these samples apparently crystallized in a one-phase region.

titions K and Ti more strongly than the Fe–Mg amphiboles.

Associated minerals and phase relations

Typical analyses of cordierite, garnet, and biotite from the Old Woman–Piute samples are presented in Table 4. Garnet analyses show considerable Mn and Ca contents (15.8 to 24 mole%combined grossular and spessartine). Staurolite±spinel, which occur only as enclaves in cordierite, never in contact with orthoamphibole, have enriched contents of Zn (Stoddard, 1979).

The distributions of Al and Mg/Fe are related systematically to the mineral assemblage (Fig. 11). The most Mg-rich specimens carry (biotite +) anthophyllite + cordierite, but not gedrite (W29D, Wan, 5A2); the most Fe-rich and Al-poor have (biotite +) garnet + gedrite + cummingtonite (5A3) or anthophyllite(?) (W127); the Al, Fe-rich sample (W223) has (biotite +) garnet + cordierite + gedrite; and an apparently compositionally intermediate specimen (5XX) has (biotite +) cordierite + anthophyllite + gedrite. A Ca-rich specimen (W29B) contains (biotite +) hornblende + cummingtonite + garnet.

TABLE 3. CLINOAMPHIBOLE ANALYSES

Sample	5A3	5A3	W29B	W29B
Grain	cum1	cum2	cum	hbl
		weight % oxides		
SiO_2	52.27	51.50	54.81	42.40
Al_2O_3	2.79	3.08	2.13	16.73
Cr_2O_3			0.05	0.19
TiO_2	0.07	0.10	0.06	0.38
FeO	23.76	23.10	21.79	16.28
MnO	0.36	0.34	0.99	0.44
MgO	17.39	16.76	18.01	9.22
CaO	0.53	0.64	0.76	10.55
Na_2O	0.25	0.28	0.22	1.67
K_2O	0.13	0.13	0.11	0.36
ZnO	0.20	0.27	0.31	0.16
total	97.75	96.21	99.24	98.18
I	site occupancy (per 23 oxygens, anhydrous)			
Si	7.675	7.675	7.846	6.232
Al^{iv}	0.325	0.325	0.154	1.768
M1,2,3,4				
Al^{vi}	0.158	0.216	0.206	1.144
Ti	0.007	0.011	0.007	0.042
Cr			0.006	0.022
Mg	3.806	3.723	3.842	2.030
Fe	2.908	2.879	2.609	2.011
Zn	0.012	0.016	0.017	0.009
Mn	0.045	0.043	0.120	0.055
Ca	0.083	0.102	0.116	1.670
Na		0.010	0.062	0.017
ΣM	7.019	7.000	6.985	7.000
A				
Na	0.072	0.071		0.463
K	0.024	0.024	0.020	0.068
ΣA	0.096	0.095	0.020	0.531

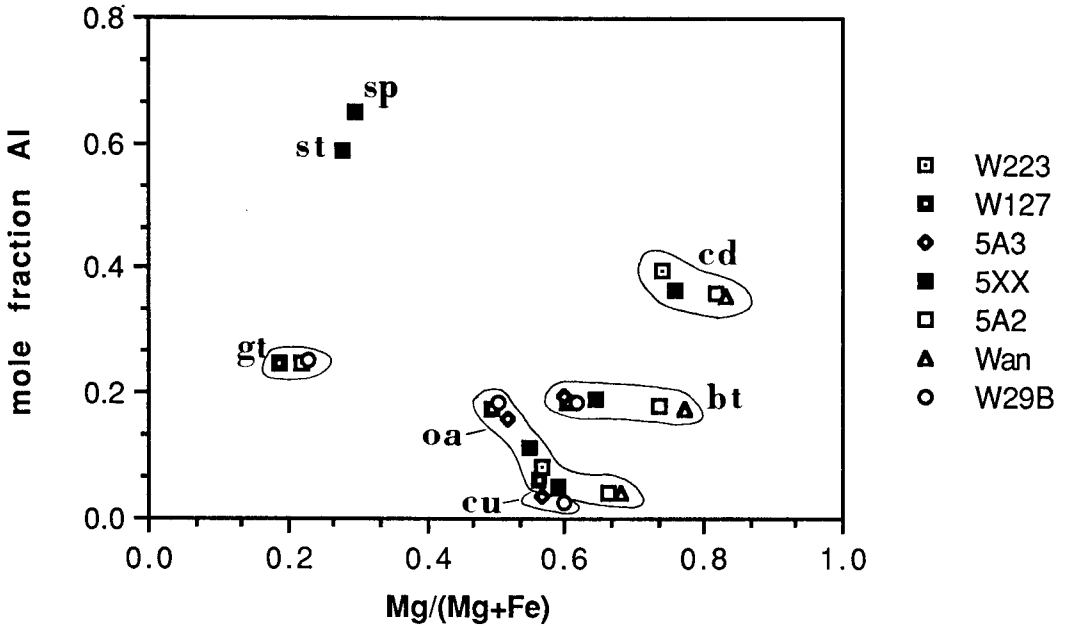

FIG. 11. Compositions of coexisting phases in orthoamphibole-bearing rocks, plotted in terms of mole fraction of Al *vs.* molar Mg/(Mg + Fe). Abbreviations: st, staurolite; sp, spinel; gt, garnet; cd, cordierite; bt, biotite; cu, cummingtonite; oa, gedrite–anthophyllite. Staurolite and spinel occur only as enclaves separated from orthoamphiboles.

The absence of the association staurolite (or aluminium silicate polymorph) + orthoamphibole implies that the Sweetwater Wash rocks underwent Cretaceous metamorphism on the high-temperature side of the simplified AFM reaction:

staurolite (or Al_2SiO_5)
+ orthamphibole → garnet + cordierite.

The relatively low Fe/Mg ratios of the orthoamphibole-bearing rocks is consistent with the occurrence of the assemblage garnet + cordierite + orthoamphibole rather than the assemblage garnet + cordierite + staurolite.

Metamorphic history and conclusions

Proterozoic metamafites from the Old Woman Mountains of the southeastern California Mojave Desert have Ca-poor, Al-rich compositions suggestive of extensive pre-metamorphic, possibly submarine, alteration. Subjected to medium- to high-temperature regional metamorphism during a Proterozoic event and then again during the Cretaceous, these rocks developed mineral assemblages dominated by low- and high-Al orthoamphiboles, cordierite, and one or more Fe–Mg–Al–(Ca) phases, including staurolite, garnet, cummingtonite, hornblende, biotite, Ca-plagioclase, corundum, and spinel.

A complex polymetamorphic history is implied by other rocks in and near Sweetwater Wash, as discussed in other studies cited above; all three Al_2SiO_5 polymorphs occur in various pelitic rocks, but each was produced at a different time. Early Proterozoic metamorphism was probably in the granulite facies (sillimanite field), as evidenced by orthopyroxene inclusions in garnet amphibolite. If orthopyroxene was present originally in the orthoamphibole-bearing rocks, it must have been consumed in subsequent reactions. A paragenetic sequence of kyanite → sillimanite → andalusite is broadly demonstrable for post-granulite metamorphism. The kyanite → sillimanite transition probably occurred during an early phase of Mesozoic regional metamorphism, with the rocks undergoing a negative dP/dT (clockwise) trajectory. The late andalusite porphyroblasts that occur in some nearby pelitic rocks undoubtedly correlate with intrusion of granitoid plutons at about 74 Ma, after the rocks had cooled substantially from peak regional metamorphic temperatures. This later event is thought to be responsible for the incipient unmixing of the orthoamphiboles.

TABLE 4. SELECTED ANALYSES OF ASSOCIATED PHASES

Sample	W223	W127	W29B	W223	W145	W127	W29B	5A2
Mineral	gar	gar	gar	crd	crd	bio	bio	bio
				weight % oxides				
SiO_2	37.75	38.58	38.14	48.05	48.21	37.87	38.18	39.22
Al_2O_3	21.50	21.52	21.74	32.58	32.65	16.50	16.69	16.51
Cr_2O_3	0.10	0.01	0.08	0.03		0.10	0.12	
TiO_2	0.05	0.05	0.09	0.02	0.03	1.27	1.10	1.28
FeO	30.33	27.44	26.98	6.08	6.18	16.55	15.70	11.14
MnO	3.14	5.62	5.16	0.14	0.17	0.10	0.16	0.05
MgO	4.77	3.58	4.47	9.77	9.27	13.91	14.08	17.23
CaO	3.20	3.90	3.11	0.09	0.08	0.26	0.09	0.09
Na_2O				0.44	0.71	0.47	0.18	0.53
K_2O				0.06	0.00	8.40	9.26	8.60
ZnO						0.59		0.00
total	100.84	100.70	99.77	97.26	97.30	96.02	95.87	94.63
cations	12 oxygens			18 oxygens		11 oxygens		
Si	2.974	3.034	3.011	4.968	4.984	2.816	2.834	2.863
Al^{iv}	0.026			1.032	1.016	1.184	1.166	1.137
Al^{vi}	1.971	1.995	2.023	2.939	2.964	0.263	0.294	0.284
Ti	0.003	0.003	0.006	0.002	0.002	0.071	0.061	0.070
Cr	0.006	0.001	0.005	0.002		0.006	0.007	
Fe^{3+}	0.020	0.001		0.057	0.034			
Mg	0.560	0.420	0.526	1.506	1.428	1.541	1.557	1.874
Fe	1.980	1.804	1.781	0.475	0.501	1.029	0.974	0.681
Zn						0.017		0.000
Mn	0.209	0.374	0.345	0.012	0.015	0.006	0.010	0.003
Ca	0.270	0.329	0.263	0.009	0.009	0.021	0.007	0.007
Na				0.087	0.143	0.068	0.026	0.075
K				0.007	0.001	0.797	0.876	0.801

Both Proterozoic and Cretaceous metamorphic events apparently attained temperatures above the crest of the solvus in the orthoamphibole series; thus supersolvus, presumably homogeneous, orthoamphiboles were initially produced. Due to both chemical differences among the rocks and to different mineral associations, the range of orthoamphiboles produced spanned the series from anthophyllite to gedrite. Orthoamphiboles from some of the rocks fall in a single-orthoamphibole field, either gedrite (W145) or anthophyllite (Wan, W29D, 5A2), while most of the other samples contained orthoamphiboles that apparently underwent at least limited exsolution during cooling from either, or possibly from both of the metamorphic events. Late Mesozoic unmixing was incomplete, of very fine, mainly submicroscopic scale, and apparently ceased at temperatures between 500 and 600°C. Rapid uplift following Mesozoic metamorphism (Hoisch *et al.*, 1988; Foster *et al.*, 1989) likely inhibited the exsolution process.

Acknowledgements

Mineral analyses were done (by EFS) at the Electron Microprobe Laboratory, Department of Earth and Space Sciences, University of California, Los Angeles, and at the Southeastern Regional Electron Microprobe Facility, located in the Department of Geological Sciences, University of South Carolina, under the direction and with the kind assistance of Bob Jones (UCLA) and Scott Vetter (U. So. Carolina). Expenses of this study were borne mainly by grants to CFM from the National Science Foundation (EAR 78–23694) and from the Vanderbilt University Research Council.

References

Bender, E. E. and Miller, C. F. (1987) Petrology of the Fenner Gneiss, a major Proterozoic metaplutonic unit in the eastern Mojave Desert, California. *Geol. Soc. Amer. Abstr. with Programs*, **19,** 358.

Berg, J. H. (1985) Chemical variations in sodium gedrite from Labrador. *Am. Mineral.* **70,** 1205–10.

Crowley, P. D. and Spear, F. S. (1981) The orthoamphibole solvus: P, T, X(Fe-Mg) relations. *Geol. Soc. Amer. Abstr. with Programs*, **13,** 435.

Foster, D. A., Harrison, T. M. and Miller, C. F. (1989) Age, inheritance, and uplift history of the Old Woman–Piute batholith, California and implications for K-feldspar age spectra. *J. Geol.* **97,** 232–43.

Gleason, J. D., Miller, C. F. and Wooden, J. L. (1988) Barrel Spring alkalic complex; 1.4-Ga anorogenic plutonism in the Old Woman–Piute Range, eastern Mojave Desert, California. *Geol. Soc. Amer. Abstr. with Programs*, **20,** 164.

Harley, S. L. (1985) Paragenetic and mineral-chemical relationships in orthoamphibole-bearing gneisses from Enderby Land, east Antarctica: A record of Proterozoic uplift. *J. Metamorphic Geol.* **3,** 179–200.

Hawthorne, F. C. (1983) The crystal chemistry of the amphiboles. *Can. Mineral.* **21,** 173–480.

Hoisch, T. D., Miller, C. F., Heizler, M. T., Harrison, T. M. and Stoddard, E. F. (1988) Late Cretaceous regional metamorphism in southeastern California. In *Metamorphism and Crustal Evolution of the Western United States* (Ernst, W. G., ed.). *Rubey Volume VII*. Prentice-Hall, Englewood Cliffs, NJ, 538–71.

Howard, K. A., John, B. E. and Miller, C. F. (1987) Metamorphic core complexes, Mesozoic ductile thrusts, and Cenozoic detachments; Old Woman Mountains–Chemehuevi Mountains transect, California and Arizona. In *Geologic diversity of Arizona and its margins: Excursions to choice areas* (Davis, G. H. and Vanderwolder, E. M., eds.) *Arizona Bur. Geol. Mineral Techn., Spec. Pap.* **5,** 365–82.

James, R. S., Grieve, R. A. F. and Pauk, L. (1978) The petrology of cordierite–anthophyllite gneisses and associated mafic and pelitic gneisses at Manitouwadge, Ontario. *Am. J. Sci.* **278,** 41–63.

Miller, C. F., Howard, K. A. and Hoisch, T. D. (1982) Mesozoic thrusting, metamorphism, and plutonism, Old Woman–Piute Range, southeastern California. In *Mesozoic–Cenozoic tectonic evolution of the Colorado River region, California, Arizona, and Nevada (Anderson-Hamilton Volume)* (Frost, E. G. and Martin, D. L., eds.). San Diego, Cordilleran Publishers, 561–81.

Reinhardt, J. (1987) Cordierite–anthophyllite rocks from north-west Queensland, Australia: Metamorphosed magnesian pelites. *J. Metamorphic Geol.* **5,** 451–72.

Robinson, P. and Jaffe, H. W. (1969) Aluminous enclaves in gedrite-cordierite gneiss from southwestern New Hampshire. *Am. J. Sci.* **267,** 389–421.

—— Ross, M. and Jaffe, H. W. (1971) Composition of the anthophyllite–gedrite series; comparisons of gedrite and hornblende, and the anthophyllite–gedrite solvus. *Am. Mineral.* **56,** 1005–41.

—— Spear, F. S., Schumacher, J. C., Laird, J., Klein, C., Evans, B. W. and Doolan, B. L. (1982) Phase relations of metamorphic amphiboles: Natural occurrence and theory. In *Amphiboles: Petrology and experimental phase relations* (Veblen, D. R. and Ribbe, P. H., eds.). *Reviews in Mineralogy*, **9B,** Mineral. Soc. Amer., 1–228.

Rock, N. M. S. and Leake, B. E. (1984) The International Mineralogical Association amphibole nomenclature scheme: computerization and its consequences. *Mineral. Mag.* **48,** 211–27.

Schumacher, J. C. and Robinson, P. (1987) Mineral chemistry and metasomatic growth of aluminous enclaves in gedrite–cordierite gneiss from southwestern New Hampshire, USA. *J. Petrol.* **28,** 1033–73.

Spear, F. S. (1980) The gedrite-anthophyllite solvus and the composition limits of orthoamphibole from the Post Pond Volcanics, Vermont. *Am. Mineral.* **65,** 1103–18.

Stoddard, E. F. (1979) Zinc-rich hercynite in high-grade metamorphic rocks: A product of the dehydration of staurolite. Ibid. **64,** 736–41.

Stone, P., Howard, K. A. and Hamilton, W. (1983) Correlation of metamorphosed Paleozoic strata of the southeastern Mojave Desert region, California and Arizona. *Geol. Soc. Amer. Bull.* **94,** 1135–47.

Stout, J. H. (1972) Phase petrology and mineral chemistry of coexisting amphiboles from Telemark, Norway. *J. Petrol.* **13,** 99–145.

Thomas, W. M., Clark, H. S., Young, E. D., Orrell, S. E. and Anderson, J. L. (1988) Proterozoic high-grade metamorphism in the Colorado River region, Nevada, Arizona, and California. In *Metamorphism and Crustal Evolution of the Western United States* (Ernst, W. G., ed.). *Rubey Volume VII*. Prentice-Hall, Englewood Cliffs, NJ, 526–37.

Treloar, P. J. and Putnis, A. (1982) Chemistry and microstructure of orthoamphiboles from cordierite-amphibole rocks at Outokumpu, North Karelia, Finland. *Mineral. Mag.* **45,** 55–62.

Vallance, T. G. (1967) Mafic rock alteration and isochemical development of some cordierite-anthophyllite rocks. *J. Petrol.* **8,** 84–96.

Young, E. D. and Wooden, J. P. (1988) Mid-crustal emplacement of Mesozoic granitoids, eastern Mojave Desert: Evidence from crystallization barometry. *Geol. Soc. Amer. Abstr. with Programs*, **20,** 244.